Journal of Organometallic Chemistry, 471 (1994) 71–76

Structures and energetics of radical cations containing tributyltin fragments: a PM3 study

Christopher Glidewell

School of Chemistry, University of St Andrews, St Andrews, Fife KY16 9ST (UK)

Christopher J. Rhodes

Department of Chemistry, Queen Mary and Westfield College, Mile End Road, London E1 4NS (UK)

(Received October 6, 1993)

Abstract

The radical cation $(Bu_4Sn)^{+\bullet}$ is shown by PM3 calculations to adopt a structure of C_s overall symmetry and approximate C_{3v} local symmetry: the positive hole is localised entirely in one Sn–C bond, which is markedly elongated, while the remaining Bu_3Sn fragment approaches planarity at tin. The radical cation $(Me_4Sn)^{+\bullet}$ is similar. Both $(Bu_3SnCMe_3)^{+\bullet}$ and $(Me_3SnCMe_3)^{+\bullet}$ have C_{3v} symmetry, again with long Sn–CMe_3 bonds and nearly planar R_3Sn fragments. In the series of radical cations $(Bu_3SnCH_2Ar)^{+\bullet}$ the positive hole is usually strongly localised in the Sn–C(benzyl) bond, which becomes longer and weaker as the electron-withdrawing capacity of the aryl substituent increases, culminating in the case of Ar = 3, 4, 5–$C_6H_2(NO_2)_3$ where the radical cation is less stable than the fragment pair Bu_3Sn^+ and $ArCH_2^\bullet$. Where the benzyl group carries a 2-nitro substituent, loss of a butyl rather than a benzyl radical is accompanied by formation of the oxometallocycle $Bu_2\overline{SnCH_2C_6H_4N(O)O}$. In both the chain-extended conformer of the amino-functionalised radical cation $[Bu_3Sn(CH_2)_3NMe_2]^{+\bullet}$, in which the tin is approximately tetrahedral, and the azametallocyclic isomer $[Bu_3\overline{Sn(CH_2)_3N}Me_2]^{+\bullet}$, which contains trigonal bipyramidal tin, the positive hole is localised in a single Sn–C bond, which is long and apical in the trigonal bipyramidal isomer.

Key words: Tin; Molecular orbital calculations; Radical cations; Electron spin resonance

1. Introduction

The electron spin resonance spectrum of matrix-isolated $(Bu_4Sn)^{+\bullet}$ radical cations, formed by γ-irradiation of dilute frozen solutions of Bu_4Sn in $CFCl_3$, shows that the positive hole is strongly confined to a single Sn–C bond [1], as in simpler radical cations $(Me_3SnR)^{+\bullet}$ [2]. When a terminal functional group was present in the butylgroups, as $(CH_2)_3NMe_2$, then the ESR spectrum of the corresponding radical cation was not observed, but only that of the butyl radical; this was interpreted [1] in terms of intramolecular cyclisation at the tin centre with concurrent expulsion of a neutral butyl radical. For the radical cations $(Bu_3SnCH_2Ar)^{+\bullet}$ the positive hole again appears [1] to be strongly confined to the unique tin–carbon bond; dissociation to form benzyl radicals is irreversible when the aryl group is phenyl but reversible when it is *p*-methoxyphenyl.

We report below the results of PM3 calculations on a range of radical cations containing tributyltin groups, together with those on appropriate molecular fragments, which provide information on the energetics and on the molecular and electronic structures of these species.

2. Calculations

All calculations were made by the PM3 method [3] as incorporated in the MOPAC system [4], version 6.0. Published atomic parameters were employed [5,6]. UHF wave functions were employed for all open-shell species, and all geometric variables were simultaneously optimised unless it is specifically stated to the

---

Correspondance to: Dr. C. Glidewell.

0022-328X/94/$7.00
SSDI 0022-328X(93)24259-8

contrary: the maximum number of independent geometric variables was 186 in $Bu_3SnCH_2C_6H_2(OCH_3)_3$ and its radical cation.

3. Results and discussion

3.1. Tetrabutyltin and its radical cation

We recently showed [7] that the PM3 method provides a rather better description than its predecessor, the MNDO method, of radical ion behaviour in the permethylated series $[M_2(CH_3)_6]^{x+/-}$ where M represents one of the elements in Periodic Groups 13–15. It seemed prudent, nevertheless, to compare as an initial step, the PM3 results for Me_4Sn and its radical cation with those obtained both from experiment and from MNDO calculations. For the neutral Me_4Sn, the optimised structure had T_d symmetry with a Sn–C bond length of 2.148 Å, significantly closer to the experimental value of 2.134 Å [8] than achieved by the MNDO calculations, 2.064 Å [9]. The ionisation energies calculated by PM3 and MNDO are 10.70 eV and 10.91 eV respectively: the reported value of 8.76 eV [10,11] for Me_4Sn differs considerably from the 10.3 eV reported [12] for Et_4Sn. Both the MNDO and PM3 calculations predict the HOMO in Me_4Sn to have T_2 symmetry, so that Jahn–Teller distortion can lead to a C_{3v} radical cation, as found experimentally [2] and by calculation. The two calculations agree in finding a single elongated Sn–C bond, 2.349 Å (MNDO) or 2.590 Å (PM3) and an almost planar Me_3Sn group with CSnC angles of 116.9° (MNDO) or 118.9° (PM3): the electronic distribution in this radical cation is clearly in the sense of $(Me_3Sn^+/CH_3^\bullet)$, consistent with the observation [2] that methyl radicals are formed upon annealing matrices containing $(Me_4Sn)^{+\bullet}$. Clearly the structure of $(Me_4Sn)^{+\bullet}$ indicates that this species is well along the

TABLE 1. Optimised molecular parameters for Bu_4Sn, its radical cation, and related species

	Skeletal point group	$\Delta H_f^\ominus$ (kJ mol^{-1})	d(SnC) (Å)	∢(CSnC) (°)
Bu_4Sn	D_{2d}	−289.6	2.185(×4)	110.3(×2) 109.1(×4)
$(Bu_4Sn)^{+\bullet}$	C_s	+544.4	2.603(×1) (a) 2.133(×1) (b) 2.128(×2) (c)	97.1(ab) 97.8(ac) 118.3(bc) 118.2(cc)
Bu_3SnCMe_3	C_{3v}	−294.1	2.221(×1) (a) 2.187(×3) (b)	109.4(ab) 109.5(bb)
$(Bu_3SnCMe_3)^{+\bullet}$	C_{3v}	+502.1	2.535(×1) (a) 2.138(×3) (b)	103.3(ab) 114.8(bb)
$Bu_3SnSnMe_3$	C_{3v}	−247.4	2.253(Sn–butyl) (a) 2.766(Sn–Sn) (b) 2.116(Sn–methyl) (c)	107.9(aa) 111.0(ab) 108.6(bc) 110.3(cc)
$(Bu_3SnSnMe_3)^{+\bullet}$	C_{3v}	+592.0	2.111(Sn–butyl) (a) 3.279(Sn–Sn) (b) 2.090(Sn–methyl) (c)	112.8(aa) 105.8(ab) 98.2(bc) 118.0(cc)
Me_4Sn	T_d	−53.6	2.148(×4)	109.5(×6)
$(Me_4Sn)^{+\bullet}$	C_{3v}	+847.2	2.590(×1) (a) 2.081(×3) (b)	95.9(ab) 118.9(bb)
Me_3SnCMe_3	C_{3v}	−101.0	2.214(×1) (a) 2.150(×3) (b)	108.7(ab) 110.2(bb)
$(Me_3SnCMe_3)^+$	C_{3v}	+696.9	2.579(×1) (a) 2.090(×3) (b)	99.3(ab) 117.4(bb)
$Me_3SnSnMe_3$	D_{3d}	−46.7	2.176(Sn–C) (a) 2.820(Sn–Sn) (b)	107.8(aa) 111.1(ab)
$(Me_3SnSnMe_3)^{+\bullet}$	D_{3d}	+792.0	2.124(Sn–C) (a) 3.418(Sn–Sn) (b)	116.6(aa) 100.8(ab)

reaction pathway to planar $(Me_3Sn)^+$ cations and free methyl radicals.

For Bu_4Sn itself, the geometry optimised to a structure of D_{2d} symmetry (Table 1) with a HOMO of E symmetry and a calculated ionisation energy of 10.09 eV. The radical cation is consequently a Jahn–Teller sensitive species, expected to distort to C_s symmetry. Consistent with this, the optimised structure of $(Bu_4Sn)^{+\bullet}$ (Table 1) does indeed reflect the localisation of the positive hole in a single Sn–C bond; one such bond is lengthened to 2.603 Å from the 2.185 Å in the neutral, while the other three such bonds have mean length 2.130 Å, midway between the values in Bu_4Sn and $(Bu_3Sn)^+$, 2.089 Å. Within the Bu_3Sn fragment of $(Bu_4Sn)^{+\bullet}$ the calculated CSnC bond angles are 118.2° and 118.3°(×2); hence the deduction from ESR data [1] that the Bu_3Sn unit in $(Bu_4Sn)^{+\bullet}$ is planar is closely supported by the present calculations.

Similar deductions of near-planar R_3Sn fragments have been made for both $(Me_3SnCMe_3)^{+\bullet}$ and $(Me_6Sn_2)^{+\bullet}$ [2], as well as for the Me_3Sn group in $(Me_4Sn)^{+\bullet}$ [2]: the present calculations again shed light on these deductions. The calculated angles CSnC within the Me_3Sn groups in $(Me_3SnX)^{+\bullet}$ for X = CH_3, CMe_3 or $SnMe_3$ are respectively 118.9°, 117.4° and 116.6°, while the corresponding angle in $(Bu_3SnCMe_3)^{+\bullet}$ is only 114.8°: at the same time, the calculated CCC angles within the CMe_3 groups in $(Me_3SnCMe_3)^{+\bullet}$ and $(Bu_3SnCMe_3)^{+\bullet}$ are 118.3° and 118.5° respectively. The charge distribution in $(Bu_3SnSnMe_3)^{+\bullet}$ is clearly in the sense $(Bu_3Sn^\bullet/SnMe_3{}^+)$, and the CSnC angles within the radicaloid Bu_3Sn and cationoid Me_3Sn fragments are 112.8° and 118.0° respectively, with the structure at the cationic tin centre again approaching planarity.

3.2. *Benzylic species Bu_3SnCH_2Ar and their radical cations*

For a wide range of aromatic groups Ar, the structures of the neutral benzylic species Bu_3SnCH_2Ar optimised to C_s symmetry, with approximate C_{3v} symmetry for the Bu_3Sn fragment, and with the aryl ring perpendicular to the mirror plane. In all cases there was a substantial localisation of the HOMO in the

TABLE 2. Principal properties of benzylic radical cations $[Bu_3SnCH_2Ar]^{+\bullet}$

Ar	$d(Sn-CH_2Ar)$ (Å)	$p(Sn-CH_2Ar)$	$D(Bu_3Sn-CH_2Ar)$ (kJ mol^{-1})	$q(Bu_3Sn)$
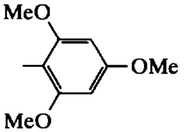	2.310	0.638	138.5	+0.383
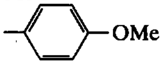	2.291	0.630	115.2	+0.413
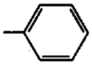	2.380	0.452	92.5	+0.565
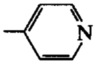	2.442	0.355	61.3	+0.655
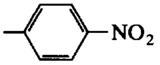	2.452	0.342	42.9	+0.670
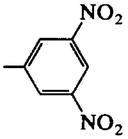	2.511	0.278	15.6	+0.734
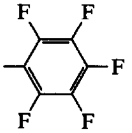	2.576	0.235	19.7	+0.777
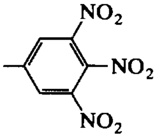	2.566	0.225	−16.0 [a]	+0.786

[a] See text.

unique Sn–C(benzyl) bond, as well as in the aryl ring, and this Sn–C contribution increased with the electron-withdrawing character of the CH_2Ar group, as judged by the net charge on the Bu_3Sn group as a whole, rather than by the charge on the tin atom only. For neutral Bu_3SnCH_2Ar systems, the calculated charge on the Bu_3Sn fragment ranges from +0.077 for $Ar = 2,4,6\text{-}(MeO)_3C_6H_2$, to +0.245 for $Ar = 2,4,6\text{-}(NO_2)_3C_6H_2$. The behaviour of these benzylic species upon ionisation has been studied for a range of substituents, and this provides some understanding of the behaviour observed experimentally [1] for the radical cations.

The important molecular parameters for a range of radical cations $[Bu_3SnCH_2Ar]^{+\bullet}$ are listed in Table 2. With a single exception, there are broad correlations between these parameters. In general, as the electron-withdrawing character of the benzyl group increases, the Sn–C(benzyl) bond in the radical cation becomes longer and weakens. The exception lies in the bond length for 2,4,6-trimethoxybenzyl, but here steric effects involving the 2,6 substituents may contribute; the bond order is nonetheless the highest in the series. At the same time the dissociation energy for the process [eqn. (1)]

$$[Bu_3SnCH_2Ar]^{+\bullet} \longrightarrow Bu_3Sn^+ + CH_2Ar^\bullet \qquad (1)$$

decreases, becoming only *ca.* 15 kJ mol^{-1} for the 3,5-dinitrobenzyl derivative: simultaneously the total net charge on the Bu_3Sn fragment steadily increases. All these trends are indicative of increasing Bu_3Sn^+ character in $[Bu_3SnCH_2Ar]^{+\bullet}$ as the supply of electrons from the benzyl substituent is diminished.

Once entropic considerations are taken into account, these trends are consistent with the observation [1] of reversible benzyl radical formation from $Bu_3SnCH_2C_6H_4OMe$, but irreversible benzyl radical formation from $Bu_3SnCH_2C_6H_5$.

A logical extension of this series, to take the energies of the isolated fragments Bu_3Sn^+ and $^\bullet CH_2Ar$ below that of $[Bu_3SnCH_2Ar]^{+\bullet}$, is to consider multiple nitro groups in the 2,4 or 6 positions. However for each of the 2,4-dinitro, 2,6-dinitro or 2,4,6-trinitro derivatives, optimisation of the radical cation geometry led to loss of a butyl radical, rather than of benzyl [eqn. (2)]:

$$[Bu_3SnCH_2Ar]^{+\bullet} \longrightarrow (Bu_2SnCH_2Ar)^+ + Bu^\bullet \qquad (2)$$

This apparent paradox, whereby tin cations $(Bu_2SnCH_2Ar)^+$ appear to be stabilised if Ar is a very strongly electron-withdrawing poly-nitrobenzyl group, is resolved by a careful inspection of the geometries of the resulting cations (Table 3). In each example, there is a strong attractive interaction between the positively-charged tin centre and one of the negatively charged oxygen atoms of the nitro group in the 2(6) position. The result of this is to render one of the N–O bonds in this nitro group rather longer and weaker than is typical in an unperturbed nitro group (such N–O is typically calculated to be 1.20–1.22 Å in length, with bond orders in the range 1.45–1.55), while the other approaches the character of a double bond, thus:

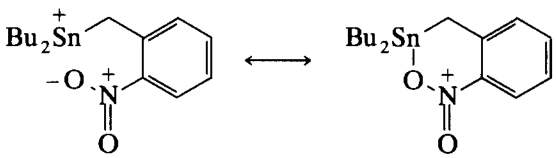

This occurs even for with a single nitro group provided it is in the 2-position.

Ring formation of this type, involving interaction of a remote oxygen atom with an electrophilic metal centre, has previously been observed for compounds of

TABLE 3. Structural parameters for oxametallacyclic cations derived from $Bu_3SnCH_2Ar)^{+\bullet}$ containing 2-nitro substituents

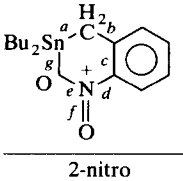

	2-nitro		2,4-dinitro		2,6-dinitro		2,4,6-trinitro	
	Distance (Å)	Bond Order	Distance (Å)	Bond Order	Distance (Å)	Bond Order	Distance (Å)	Bond Order
a	2.126	0.812	2.128	0.801	2.155	0.786	2.131	0.781
b	1.484	1.003	1.477	1.018	1.477	1.023	1.472	1.031
c	1.413	1.328	1.418	1.296	1.408	1.322	1.420	1.308
d	1.458	0.990	1.464	0.969	1.471	0.955	1.472	0.955
e	1.279	1.159	1.286	1.145	1.275	1.188	1.282	1.160
f	1.194	1.702	1.188	1.746	1.191	1.720	1.188	1.749
g	2.067	0.376	2.072	0.410	2.135	0.347	2.083	0.389

antimony [13], germanium [14], and bismuth [15], and well as tin [16,17].

For highly electron-withdrawing benzyl groups that cannot form such oxametallacycles, such as $CH_2C_6F_5$, the trend towards long weak Sn–C(benzyl) bonds is continued. For the 3,4,5-trinitrobenzyl compound, the radical cation is actually of higher energy, by some 16 kJ mol^{-1}, than the isolated fragments Bu_3Sn^+ and $ArCH_2^\bullet$, but is separated from them by an energy barrier of 19.7 kJ mol^{-1} which occurs at a Sn–C(benzyl) distance of *ca*. 3.4 Å.

In every case considered in which Sn–C(benzyl) bond elongation is the preferred relaxation pathway upon radical cation formation (*i.e* all except those species containing a nitro group in the phenyl 2-position) the calculated spin densities at the benzylic CH_2 group show marked differences between those in $[Bu_3SnCH_2Ar]^{+\bullet}$ and those in $ArCH_2^\bullet$, with the $ArCH_2^\bullet$ couplings calculated typically to be two to three times those in the intact radical cation. Although for most species dissociation according to eqn. (1) is endothermic, there will always be an excess of energy present in radical cations generated by electron transfer to $(CFCl_3)^{+\bullet}$ [1]. The trend in properties apparent from the data of Table 2 thus affords a satisfactory rationalisation for the observed behaviour [1] of the radical cations derived from Bu_3SnCH_2Ph and $Bu_3SnCH_2C_6H_4OMe$.

3.3. $Bu_3Sn(CH_2)_3NMe_2$ and its radical cation

While formation of oxametallacycles accompanying loss of butyl radicals has not yet been observed for 2-nitrobenzyltin radical cations, analogous formation of an azametallacycle has been observed [1] for the radical cation of the terminally functionalised tetra-alkyl $Bu_3Sn(CH_2)_3NMe_2$.

Optimisation of the structure of $Bu_3Sn(CH_2)_3NMe_2$ shows that the $(CH_2)_3NMe_2$ substituent has the extended conformation with the HOMO strongly localised on the nitrogen atom; MNDO calculation leads to the same conclusion. Experimental ionisation energy data on R_3N and R_4Sn [10–12,18,19] suggest that these species have fairly similar ionisation energies, although the experimental data for R_4Sn do not appear to be entirely consistent. However, contrary to the assumptions of Koopmans' theorem, adiabatic ionisation of this extended conformer of $Bu_3Sn(CH_2)_3NMe_2$ leads to a radical cation for which the calculated SOMO is concentrated not on the nitrogen atom, as expected, but in a single Sn–C bond. This is entirely consistent with the earlier suggestion [1] that the electron loss upon radical cation formation occurs at the tin centre.

After extensive exploration of the conformation of the radical cation $[Bu_3Sn(CH_2)_3NMe_2]^{+\bullet}$, two energy minima were located. The global minimum, $\Delta H_f^\ominus = +472.4$ kJ mol^{-1}, corresponded to the extended conformation (**1**) of the $(CH_2)_3NMe_2$, as found also for the neutral $Bu_3Sn(CH_2)_3NMe_2$, as well as for the butyl groups: in this conformer, the tin centre is approximately tetrahedral, and the Sn–C bond lengths are all in the range 2.19–2.21 Å, while the Sn ⋯ N distance is 4.091 Å. Only 1 kJ mol^{-1} higher in energy, and separated by only a modest energy barrier (about 50 kJ mol^{-1}) is a second minimum, corresponding to an azametallacycle with approximately trigonal bipyramidal tin: the apical Sn–N distance is 2.432 Å, and the apical Sn–C distance is 2.827 Å, while the equatorial Sn–C distances are in the range 2.15–2.17 Å. This configuration at the tin centre thus represents the classic S_N2-type intermediate with apical entry and apical departure.

In the trigonal bipyramidal isomer **2** the apical bond orders are: Sn–N, 0.526 and Sn–C, 0.091, while the equatorial Sn–C bond orders γ are in the range 0.91–0.93. Clearly, departure of the apical butyl group is nearly complete, although this minimum is 17.5 kJ mol^{-1} below the energies of the separated fragments, **3** and the butyl radical.

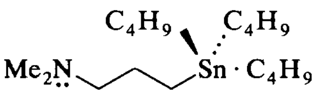

(**1**)

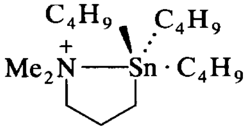

(**2**)

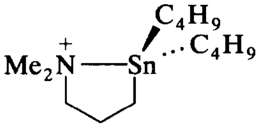

(**3**)

Consistent with, and supporting, the description of an almost completely dissociated apical butyl group in isomer **2** is the form of the SOMO in **2**, localised almost entirely on the α-carbon atom of the apical butyl group; moreover, the sum of the bond angles subtended at this carbon atom by its two attached hydrogen atoms and by the β-carbon is 356.2°, indicative of a nearly planar α-carbon remote from the tin centre. Consistent with this, the calculated spin densities for the apical butyl group in **2** are almost identical with the calculated spin densities in an isolated butyl radical. This finding makes it improbable that a distinction could be made by ESR spectroscopy alone between formation of **2** and formation of **3** plus a free butyl radical. On the other hand, the excess energy from formation **1** by electron exchange with $(CFCl_3)^{+\bullet}$ will almost certainly be sufficient to drive the reaction towards complete loss of butyl radicals, a process which may be summarised in eqn. (3):

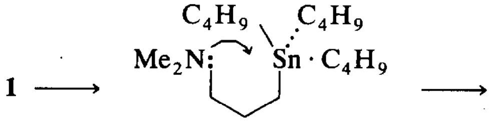

$$2 \longrightarrow 3 + C_4H_9^{\bullet} \quad (3)$$

This mechanism, indicated by the calculations, is thus in complete agreement with that suggested earlier on the basis of ESR observations [1].

References

1 E. Butcher, C.J. Rhodes, M. Standing, R.S. Davidson and R. Bowser, *J. Chem. Soc., Perkin Trans. 2*, (1992) 1469.
2 A. Hasegawa, S. Kaminaka, T. Wakabayashi, M. Hayashi, M.C.R. Symons and J. Rideout, *J. Chem. Soc., Dalton Trans.*, (1984) 1667.
3 J.J.P. Stewart, *J. Comp. Chem.*, *10* (1989) 209.
4 J.J.P. Stewart, *J. Comp.-aided Mol. Design*, *4* (1990) 1.
5 J.J.P. Stewart, *J. Comp. Chem.*, *10* (1989) 221.
6 J.J.P. Stewart, *J. Comp. Chem.*, *12* (1991) 320.
7 C. Glidewell, *J. Organomet. Chem.*, *461* (1994) 15.
8 H. Fujii and M. Kimura, *Bull. Chem. Soc. Jpn.*, *44* (1970) 2643.
9 M.J.S. Dewar, G.L. Grady and J.J.P. Stewart, *J. Am. Chem. Soc.*, *106* (1984) 6771.
10 M.F. Lappert, J. Simpson and T.R. Spalding, *J. Organomet. Chem.*, *17* (1969) P1.
11 A.L. Yergey and F.W. Lampe, *J. Organomet. Chem.*, *15* (1968) 339.
12 J.J. de Ridder and G. Dijkstra, *Rec. Trav. Chim.*, *86* (1967) 737.
13 G. Ferguson, C. Glidewell, I. Gosney, D. Lloyd, S. Metcalfe and H. Lumbroso, *J. Chem. Soc., Perkin Trans., 2*, (1988) 1829.
14 C. Glidewell, D. Lloyd and N. Wiberg, *Struct. Chem.*, *1* (1990) 151.
15 G. Ferguson, B. Kaitner, C. Glidewell and S. Smith, *J. Organomet. Chem.*, *419* (1991) 283.
16 B. Jousseaume, P. Villeneuve, M. Dräger, S. Roller and J.M. Chezeau, *J. Organomet. Chem.*, *349* (1988) C1.
17 T.A.K. Al-Allaf, U. Kobs and W.P. Neumann, *J. Organomet. Chem.*, *373* (1989) 29.
18 J. Watanabe and J.R. Mottl, *J. Chem. Phys.*, *26* (1957) 1773.
19 A.B. Cornford, D.C. Frost, F.G. Herring and C.A. McDowell, *Can. J. Chem.*, *49* (1971) 1135.